Journal of the American Heart Association

ORIGINAL RESEARCH

Antenatal Hypoxia Affects Pulmonary Artery Contractile Functions via Downregulating L-type Ca^{2+} Channels Subunit Alpha1 C in Adult Male Offspring

Huan Li, MD*; Bingyu Ji, MD*; Ting Xu, PhD*; Meng Zhao, MD; Yingying Zhang, PhD; Miao Sun, PhD; Zhice Xu, PhD; Qinqin Gao, PhD

BACKGROUND: Antenatal intrauterine fetal hypoxia is a common pregnancy complication that has profound adverse effects on an individual's vascular health later in life. Pulmonary arteries are sensitive to hypoxia, but adverse effects of antenatal hypoxia on pulmonary vasoreactivities in the offspring remain unknown. This study aimed to determine the effects and related mechanisms of antenatal hypoxia on pulmonary artery functions in adult male offspring.

METHODS AND RESULTS: Pregnant Sprague-Dawley rats were housed in a normoxic or hypoxic (10.5% O_2) chamber from gestation days 10 to 20. Male offspring were euthanized at 16 weeks old (adult offspring). Pulmonary arteries were collected for vascular function, electrophysiology, target gene expression, and promoter methylation studies. In pulmonary artery rings, contractions to serotonin hydrochloride, angiotensin II, or phenylephrine were reduced in the antenatal hypoxic offspring, which resulted from inactivated L-type Ca^{2+} channels. In pulmonary artery smooth muscle cells, the basal whole-cell Ca^{2+} currents, as well as vasoconstrictor-induced Ca^{2+} transients were significantly reduced in antenatal hypoxic offspring. In addition, increased promoter methylations within L-type Ca^{2+} channel subunit alpha1 C were compatible with its reduced expressions.

CONCLUSIONS: This study indicated that antenatal hypoxia programmed long-lasting vascular hypocontractility in the male offspring that is linked to decreases of L-type Ca^{2+} channel subunit alpha1 C in the pulmonary arteries. Antenatal hypoxia resulted in pulmonary artery adverse outcomes in postnatal offspring, was strongly associated with reprogrammed L-type Ca^{2+} channel subunit alpha1 C expression via a DNA methylation-mediated epigenetic mechanism, advancing understanding toward the effect of antenatal hypoxia in early life on long-term vascular health.

Key Words: antenatal hypoxia ■ Cav1.2 ■ male offspring ■ vascular hypocontractility

Developing embryos or fetuses can be highly sensitive to environmental insults, which can permanently alter the functions of organs, resulting in diseases later in life.[1,2] Oxygen is an essential nutrient for the fetus and placenta.[3,4] During normal pregnancy, oxygen levels within the uterus change dramatically.[3,4] Oxygen levels at the site of embryo implantation and placenta formation are low, whereas higher intrauterine oxygen levels are evident and indispensable following placenta establishment.[3–5] Hypoxia is one of the most common pathological processes for developmental fetus. When the pregnant woman has anemia, preeclampsia, heart disease, pulmonary heart disease, or placental insufficiency, intrauterine infection, umbilical cord twist, and so on can lead to fetal hypoxia in utero.[3,6] Chronic intrauterine fetal hypoxia affects

Correspondence to: Qinqin Gao, PhD, and Zhice Xu, PhD, Institute for Fetology, First Hospital of Soochow University, Suzhou 215006, P. R. China. E-mail: jennyqgao@126.com; xuzhice@suda.edu.cn

*H. Li, B. Ji, and T. Xu contributed equally.

Supplementary Material for this article is available at https://www.ahajournals.org/doi/suppl/10.1161/JAHA.120.019922

For Sources of Funding and Disclosures, see page 12.

JAHA is available at: www.ahajournals.org/journal/jaha

CLINICAL PERSPECTIVE

What Is New?

- Antenatal hypoxia damages pulmonary artery contractile functions in adult offspring.
- Pulmonary artery contractile functional disorders were associated with downregulated L-type Ca^{2+} channel subunit alpha1 C in adult offspring.

What Are the Clinical Implications?

- Our findings provide new insight into the pathological characteristics and underlying mechanisms of pulmonary vascular problems in antenatal hypoxic adult offspring.
- This new and important information may be helpful in understanding the pathophysiological development of pulmonary artery problems of the individuals who suffered from antenatal hypoxia.

Nonstandard Abbreviations and Acronyms

5-AZA	5-AZA-2'-deoxycytidine
5-HT	serotonin hydrochloride
Cav1.2	L-type Ca^{2+} channel subunit alpha1 C
IP3	inositol-1,4,5-triphosphate
LTCCs	L-type Ca^{2+} channels
PKC	protein kinase C
ROCK	Rho/Rho-kinase
siRNA	small interfering RNA

fetal development and is commonly associated with intrauterine growth restriction.[7] Our previous studies on animal models indicated that antenatal hypoxia is not only accompanied by fetal growth restriction but can also predispose offspring to vascular dysfunction in later life.[8–11] Fetal lungs are not fully developed until after birth, which means that the effects of hypoxia on lung development in late pregnancy cannot be ignored. However, no study has yet determined the effect of antenatal hypoxia on pulmonary circulation in the offspring.

Pulmonary circulation is maintained in a low-pressure, low-resistance state with little resting tone under normal physiological conditions. Pulmonary arteries (PAs) are thin-walled and rely heavily on distention for reducing PA vascular resistance when cardiac output is elevated. Under pathophysiological conditions, pulmonary vasoconstriction leads to enhanced vascular resistance and subsequent pulmonary hypertension.[12,13] Therefore, small resistance PAs are very important for blood flow regulation in the pulmonary vascular bed under both physiological and pathological conditions. Pulmonary vasoconstriction is a consequence of a rise in cytosolic free Ca^{2+} concentration in PA smooth muscle cells.[14,15] Cytosolic free Ca^{2+} concentration can be caused by release of Ca^{2+} from internal storage sites, such as sarcoplasmic reticulum or influx of Ca^{2+} from extracellular fluid through voltage-dependent Ca^{2+} channels, receptor-operated Ca^{2+} channels, or store-operated Ca^{2+} channels.[16] Voltage-dependent Ca^{2+} channels are the main Ca^{2+} channels and can be divided into 6 different subtypes based on their functional characteristics. Commonly, voltage-gated L-type Ca^{2+} channels (LTCCs) serve as the major route of extracellular Ca^{2+} influx to trigger vascular smooth muscle cell contraction.[16–18] Changes in the expressions or functions of LTCCs play an important role in the regulation of vascular tone and development of vascular dysfunction.[19,20] In addition, studies to date indicated that vascular LTCCs are likely vulnerable and sensitive to antenatal insults.[20,21] Recently, a number of studies in laboratory animals have indicated that antenatal hypoxia impaired offspring vascular contractility in small resistance arteries, such as the mesenteric and middle cerebral arteries.[8,9] However, no study so far has investigated the effect of antenatal hypoxia on pulmonary vasculature in the offspring. We therefore hypothesized that antenatal hypoxia-perturbed LTCC signaling in PAs eventually led to long-term outcomes in vascular contractility dysfunction in the offspring.

METHODS

According to the Transparency and Openness Promotion Guidelines, the data of this study are available from the corresponding author upon reasonable request. The authors declare that all supporting data are available within this article as well as in the online-only Data Supplement or from the corresponding author on request.

Experimental Animals

Pregnant Sprague–Dawley rats from the Animal Center of Soochow University were housed in a temperature-controlled room with a 10:14-hour light-dark cycle, provided with standard rat food and tap water. They were randomly divided into the control group (21% oxygen) and hypoxia group (10.5% oxygen) from gestational days 10 to 20 (N=15 per group). Hypoxia was induced by a mixture of nitrogen gas and air in an individual chamber.[11] The flow of nitrogen was adjusted to bring the percentage of oxygen to 10.5%, which was continuously monitored with an oxygen analyzer. Rats in the control group were

housed with room air flowing through chambers. All animals were fed with standard rat food and tap water throughout pregnancy. At term (gestational day 20), pregnant rats were kept in the normal environment and allowed to give birth naturally. Upon weaning, male pups were separated and provided with normal food and water and were tested at 16 weeks old. One male from each litter was used in each experimental setup. Approval of the Institutional Review Board of Soochow University was obtained for this study. The Animal Care and Use Committee of Soochow University approved this study, and all animal procedures followed the *Guidelines of the Care and Use of Laboratory Animals*.

Hemodynamic and Histologic Measurements

Right ventricular systolic pressure and PA pressure of adult male offspring were measured with cardiac catheterization as previously described.[22] Rats were anesthetized with 3% isoflurane inhalation. After anesthesia, right ventricular systolic pressure and pulmonary artery pressure of rats were measured using a Mikro-Tip pressure catheter (Millar Instruments, Houston, TX) through direct puncture of the right ventricle, followed by advancing the catheter into the main PA, using an open-chest approach. At the end of pressure measurement, blood samples were collected for measuring blood oxygen partial pressure, carbon dioxide partial pressure, lactate, hematocrit, and pH on a GEM Premier 3000 blood gas analyzer (Instrumentation Laboratory, Bedford, MA). After the hemodynamic measurement, the animals were euthanized. PA specimens were immediately collected and fixed with formaldehyde and then embedded in paraffin. PA cross sections were subjected to hematoxylin and eosin staining. The images of 10 vessels with 200 to 400 μm outside diameter in each group were taken to measure wall thickness using Image-Pro 6.0 software.

Measurement of Vascular Tone

Adult male offspring were euthanized (anesthesia with 3% isoflurane inhalation), and lungs en bloc were isolated. The PA (≈300 μm diameter) was rapidly excised and placed in ice-cold physiological saline solution, containing (mmol/L: NaCl, 126; KCl, 5; $NaHCO_3$, 14.9; KH_2PO_4, 1.2; $MgSO_4{\cdot}7H_2O$, 1.7; $CaCl_2{\cdot}2H_2O$, 2.8; EDTA, 0.025; glucose, 5.0; and HEPES, 10.0; pH 7.4 [adjusted with NaOH], gassed continuously with 5% CO_2 in O_2). Isolated PA rings (3–4 mm in length) were carefully threaded onto two 40-μm-diameter stainless steel wires and mounted in a multimyograph system for recording of isometric tension (PowerLab 16/SP with Chart 5).[11] PA rings were adjusted to maintain a suitable passive force and equilibrated for 60 minutes; then potassium chloride (KCl, 120 mmol/L) was used to achieve optimal resting tension before adding drugs. Vessel constrictions to drugs were evaluated by measuring the maximum peak and expressed as percentage of maximal tension achieved to KCl. The vessel rings were contracted with cumulatively increasing concentrations of serotonin hydrochloride (5-HT, 10^{-9}–10^{-4} mol/L), angiotensin II (10^{-11}–10^{-5} mol/L), phenylephrine (10^{-9}–10^{-4} mol/L), or BayK8644 (an agonist for voltage-dependent Ca^{2+} channels; 10^{-11}–10^{-4} mol/L). GF109203X (PKC [protein kinase C] antagonist, 10^{-6} mol/L), 2-aminoethyl diphenylborinate (inositol-1,4,5-triphosphate [IP3] receptor inhibitor, 10^{-5} mol/L), Y27632 (Rho/Rho-kinase [ROCK] inhibitor, 10^{-6} mol/L), fasudil (ROCK inhibitor, 10^{-6} mol/L), mibefradil (antagonist for L- and T-type calcium channels, 10^{-5} mol/L), or nifedipine (antagonist for LTCCs, 10^{-6} mol/L) were used for pretreating segments for 30 to 60 minutes before application of 5-HT or angiotensin II as reported.[9] In 5-AZA (5-AZA-2'-deoxycytidine; DNA methyltransferase inhibitor) treatment studies, PA rings from antenatal offspring were incubated with or without 5-AZA (10^{-6} mol/L; Sigma-Aldrich, St. Louis, MO) for 6 hours, and then vessel rings were contracted with cumulatively increasing concentrations of vascular agonists.

Electrophysiological Measurements

PAs were first dissected gently and cut into small fragments in oxygenated ice-cold Ca^{2+}-free physiological saline solution. Isolation of PA myocytes was performed as described before.[23] Briefly, the fragments were incubated with 5 mL of physiological saline solution, containing 4 mg/mL of papain, 2 mg/mL of albumin bovine V, and 1 mg/mL of dithiothreitol for ≈30 minutes in 37°C. Then the supernatant fluid was removed, tissue fragments were washed by 5 mL of oxygenated ice-cold physiological saline solution 3 times. Single myocytes were obtained by gentle trituration with a wide-bore glass pipette stored at 4°C and used within 4 hours. A conventional whole-cell patch clamp was used to record LTCCs as described before.[23] After obtaining basal whole-cell Ca^{2+} currents, nifedipine (10^{-6} mol/L) or BayK8644 ($5{\times}10^{-6}$ mol/L) were added independently in the organ bath to test the possible changes of LTCCs between the 2 groups. Patch-clamp experiments were performed using Axon700B amplifier and Clampfit 10.1 software (Axon Instruments, Foster City, CA). All recording currents were digitized with a Digidata 1440A interface (Axon Instruments), which sampled at 10 kHz and filtered at 2 kHz. Suited pipette resistance was 3 to 5 MΩ, which was obtained

from the borosilicate glass by using the horizontal pipette puller (P-97, Sutter Instrument Corp., Novato, CA), and only the seal resistances >2 GΩ, the recordings were analyzed. Current amplitudes were normalized by its membrane capacitance to get the current density, which was expressed in pA/pF, calculated as the ratio of current amplitudes to membrane capacitance. All experiments were performed at room temperature.

Cellular Ca^{2+} Imaging

Confocal Ca^{2+} imaging of myocytes was performed as described before.[24] Briefly, isolated PA myocytes were incubated with Fluo-3 AM (10^{-6} mol/L; Invitrogen, Carlsbad, CA) in Tyrode's solution, containing (mmol/L: NaCl, 135; KCl, 4.7; $CaCl_2$, 1.8; $MgCl_2$, 1; HEPES, 10; $NaH_2PO_4{\cdot}2H_2O$, 1.2; and glucose, 10; pH 7.36 [adjusted with NaOH]) for 20 minutes at room temperature. After loading, myocytes were washed 3 times with Tyrode's solution and transferred to a recording chamber. Representative single-myocyte images and traces of Ca^{2+} responses to 5-HT (10^{-4} mol/L), angiotensin II (10^{-5} mol/L), or BayK8644 (10^{-4} mol/L) were measured with a total internal reflection fluorescence microscopy electron-multiplying charge-coupled device imaging system. Nifedipine (10^{-6} mol/L) were used for pretreating myocytes for 30 to 60 minutes before application of 5-HT or angiotensin II. All images were processed and analyzed using Fiji software (Olympus, Japan). The fluorescence intensity was calculated as F/F0, where F0 is the fluorescence intensity during a period from the beginning of the recording when there was no Ca^{2+} activity, and F is the fluorescence intensity for the region of interest.

Quantitative Real-Time Polymerase Chain Reaction and Western Blot

Total RNA was isolated from the PA tissue or myocytes using Trizol reagent, and then reversed transcribed using the first-strand cDNA Synthesis Kit (Invitrogen). Real-time polymerase chain reaction was conducted using SYBR Green I master mix (Maxima SYBR Green/ROX qPCR Master Mix [2X], Thermo Scientific, Waltham, MA). Each sample was run in duplicate in 25 mL of reaction mixture. The ΔΔCt method was used to comparatively quantify the abundance of mRNA levels. The primer sequences are listed in Table S1. The protein abundance in PA was assessed by Western blot normalized to β-actin. Antibodies for Cav1.2 (SAB1402709, 1:1000) and β-actin (A5441, 1:3000) were from Sigma-Aldrich. All experiments were repeated 6 times with independently prepared tissue and performed as previously described.[25,26]

Targeted Bisulfite Sequencing

Genomic DNA was extracted from the PA tissue by the standard phenol/chloroform technique and subjected to bisulfite conversion using EZ DNA Methylation-GOLD Kit (Zymo Research, Irvine, CA) according to the manufacturer's protocols. DNA was quantified and then diluted to a working concentration of 10 to 20 ng/μL for BiSulfite Amplicon Sequencing.[25,26] CpG islands located in the proximal *Cav1.2* promoter were selected according to the following criteria: (1) ≥200 bp length; (2) ≥50% guanine-cytosine content; (3) ≥60% ratio of observed/expected dinucleotide CpG. The primer sequences are listed in Table S1. After polymerase chain reaction amplification, products were sequenced by Hiseq 2000 (Illumina, San Diego, CA). Methylation level at each tested CpG site was calculated as the percentage of the methylated cytosines over the total tested cytosines.

Cell Culture and RNA Interference Assay

Primary smooth muscle cells were enzymatically obtained from PA of control adult male offspring as previously described.[22] Briefly, deendothelialized PA was rapidly excised and placed in PBS, then cut into small pieces and added to an enzyme solution consisting 0.25% collagenase type 2. After enzyme digestion, the samples were vigorously vortexed. PA myocytes were then precipitated, resuspended, and cultured in DMEM supplemented with 12% fetal bovine serum, streptomycin (100 mg/mL), and 100 U/mL penicillin at 37°C under a humidified atmosphere of 95% air and 5% CO_2. In small interfering RNA (siRNA) transfection assay, cells were transfected twice at 24 hours intervals with the indicated siRNA using Lipofectamine 2000 (Invitrogen) following the manufacturer's instructions. siRNA duplexes for silencing Cav1.2 were synthesized by Genepharma (GenePharma, Shanghai, China). Sequences of the siRNAs were listed in Table S1. After transient transfection for 48 hours, myocytes were harvested for quantitative real-time polymerase chain reaction and Ca^{2+} imaging assays.

Statistical Analysis

Data were expressed as mean±SEM. Data were analyzed by Student *t* test or 2-way ANOVA followed by Bonferroni posttests using Prism version 7.0 (GraphPad Software, San Diego, CA). Results with a $P<0.05$ were considered as statistically significant.

RESULTS

Vascular Contractility in PA Rings

For adult male offspring, there were no significant differences in body weight (Figure S1A), lung

weight (Figure S1B), blood values (Table S2), right ventricular systolic pressure (18.19±1.96 versus 18.69±1.35 mm Hg; *P*=0.8296), and mean pulmonary artery pressure (16.64±1.13 versus 16.99±0.86 mm Hg; *P*=0.6233) between the 2 groups (Figure 1A). To determine the changes of PA contractility, vascular function assay was conducted on PA rings. PA rings used in the 2 groups had similar wall thickness and vessel diameter (Figure S1C through S1E). There were no differences of the KCl-induced maximal response between the 2 groups (Figure 1B). The PA vessels from antenatal hypoxic offspring were significantly insensitive to accumulative doses of 5-HT, angiotensin II, or phenylephrine with lower maximal response and pD2 (–log[50% effective concentration]) as compared with the control (Figure 1C and 1D, Figure S2A and S2B). Antenatal hypoxia did not decrease expressions of receptors of 5-HT, angiotensin II, or phenylephrine in

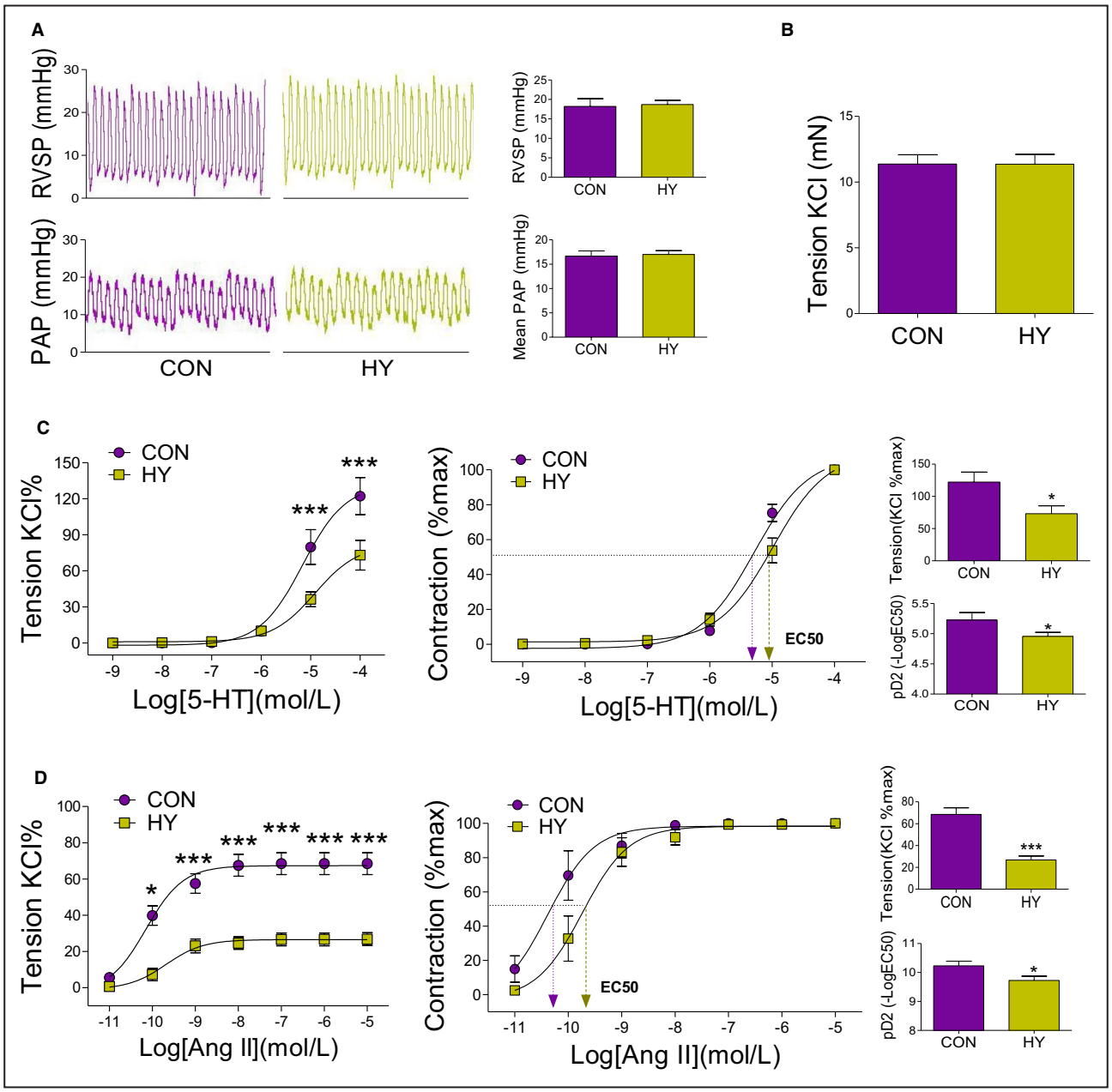

Figure 1. Vascular contractility in pulmonary artery (PA) rings.
A and **B**, Representative tracings and statistics of right ventricular systolic pressure (RVSP) and pulmonary arterial pressure (PAP) in offspring (N=5). **B**, KCl-mediated vasoconstriction (N=5, n=10). **C**, Serotonin hydrochloride (5-HT)-induced contraction and EC_{50} in the offspring PA rings (N=6, n=12). **D**, Angiotensin II (Ang II)-induced contraction and EC_{50} in the offspring PA rings (N=6, n=12). Data were presented as means±SEM. N, number of adult male offspring from different litters of each group; n, number of PA rings. Data were analyzed by Student *t* test or 2-way ANOVA followed by Bonferroni posttests. **P*<0.05; ****P*<0.001. CON indicates control group; and HY, hypoxia group.

the offspring PA (Figure S3A through S3C). These data indicated that antenatal hypoxia decreased vascular agonist-mediated PA reactivity in the adult offspring.

Antenatal Hypoxia Decreased Vascular Contractility Independent of PKC, IP3, and RhoA/Rho Kinase Pathway

Vasoconstriction is activated and maintained by both Ca^{2+}-dependent and Ca^{2+}-independent mechanisms.[27,28] In vascular myocytes, agonist receptor produces IP3 and diacylglycerol within seconds.[27,28] IP3 binds to its receptors on sarcoplasmic reticulum, allows Ca^{2+} efflux, and subsequently stimulates extracellular Ca^{2+} influx into the cytoplasm.[27,28] Ca^{2+} activates myosin light-chain kinase, which phosphorylates myosin light chain and causes myocyte contraction.[28] Agonist-receptor activation also induces myocyte contraction via the activating PKC pathway.[29,30] PKC activation can phosphorylate CPI17 (protein phosphatase 1 regulatory inhibitor), which in turn inhibits myosin light-chain phosphatase, increases myosin light-chain phosphorylation and enhances myocyte contraction.[29,30] To reveal the mechanisms underlying the vascular hypocontractility in antenatal hypoxic offspring PA, we determined the role of PKC or IP3-Ca^{2+} pathways in vascular agonist-decreased vasoconstrictions. After pretreatment with GF109203X (PKC inhibitor), 5-HT– or angiotensin II–mediated vasoconstrictions were also significantly lower in the antenatal hypoxia group (Figure 2A and 2B). Although 2-aminoethyl diphenylborinate (IP3 receptor

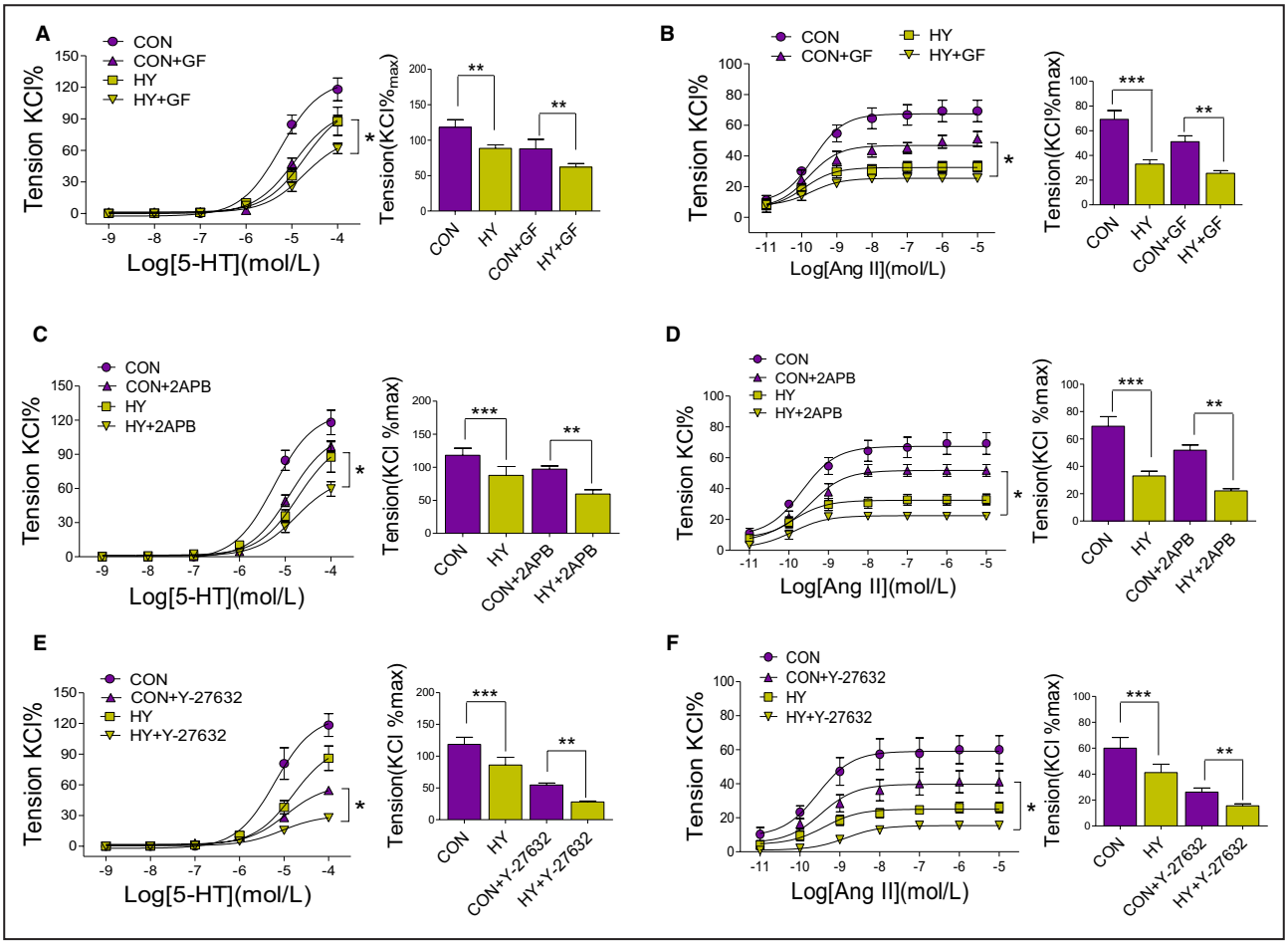

Figure 2. Antenatal hypoxia decreased vascular contractility independent of PKC (protein kinase C) inositol-1,4,5-triphosphate (IP3) and RhoA/Rho kinase pathway.
A and **B**, Serotonin hydrochloride (5-HT) or angiotensin II (Ang II)-induced contractions in the presence or absence of GF (GF109203X, PKC antagonist) in offspring pulmonary artery (PA) rings (N=6, n=12). **C** and **D**, 5-HT or Ang II–induced contractions in the presence or absence of 2APB (2-aminoethyl diphenylborinate, IP3 receptor inhibitor) in offspring PA rings (N=6, n=12). **E** and **F**, 5-HT or angiotensin II–induced contractions in the presence or absence of Y-27632 (Rho/Rho-kinase inhibitor) in offspring PA rings (N=5, n=10). Data were presented as means±SEM. N, number of adult male offspring from different litters of each group; n, number of PA rings. Data were analyzed by Student *t* test or two-way ANOVA followed by Bonferroni posttests. **P*<0.05; ***P*<0.01; ****P*<0.001. CON indicates control group; and HY, hypoxia group.

inhibitor) inhibition could produce attenuation of vascular contractility, 5-HT– or angiotensin II–mediated vasoconstrictions were also significantly lower in the antenatal hypoxia group (Figure 2C and 2D). In addition, the RhoA/ROCK pathway is one classical Ca^{2+}-independent contraction pathway and has an important role in the regulation of vascular contractility.[31] Y27632 and fasudil are inhibitors of ROCK. After pretreatment with Y27632 or fasudil, 5-HT– or angiotensin II–mediated vasoconstrictions were still significantly lower in antenatal hypoxia group (Figure 2E and 2F, Figure S4A and S4B). Meanwhile, there were no differences in expressions of ROCK isoforms (ROCK 1 and 2) and RhoA (Figure S4C). These data together indicated that antenatal hypoxia decreased offspring PA reactivity independent of PKC, IP3, and RhoA/ROCK pathway.

Antenatal Hypoxia-Decreased Vascular Contractility Was Correlated With LTCCs

After pretreatment with mibefradil (antagonist for L- and T-type Ca^{2+} channels,) or nifedipine (LTCC inhibitor), no significant differences were observed in 5-HT–, angiotensin II– or phenylephrine-mediated vasoconstrictions between the 2 groups (Figure 3A through 3D, Figure S4D). Meanwhile, no significant differences were observed in the inhibited values (mibefradil-inhibited tension subtracts that nifedipine-inhibited tension) on 5-HT– or angiotensin II–induced maximal contractions (Figure 3E). In addition, BayK8644 (voltage-dependent Ca^{2+} channel agonist) elicited lower dose-dependent vasoconstrictions in the hypoxia group, but with similar EC_{50} between the 2 groups (Figure 3F). These data together indicated that antenatal hypoxia-decreased vascular contractility was correlated to LTCCs.

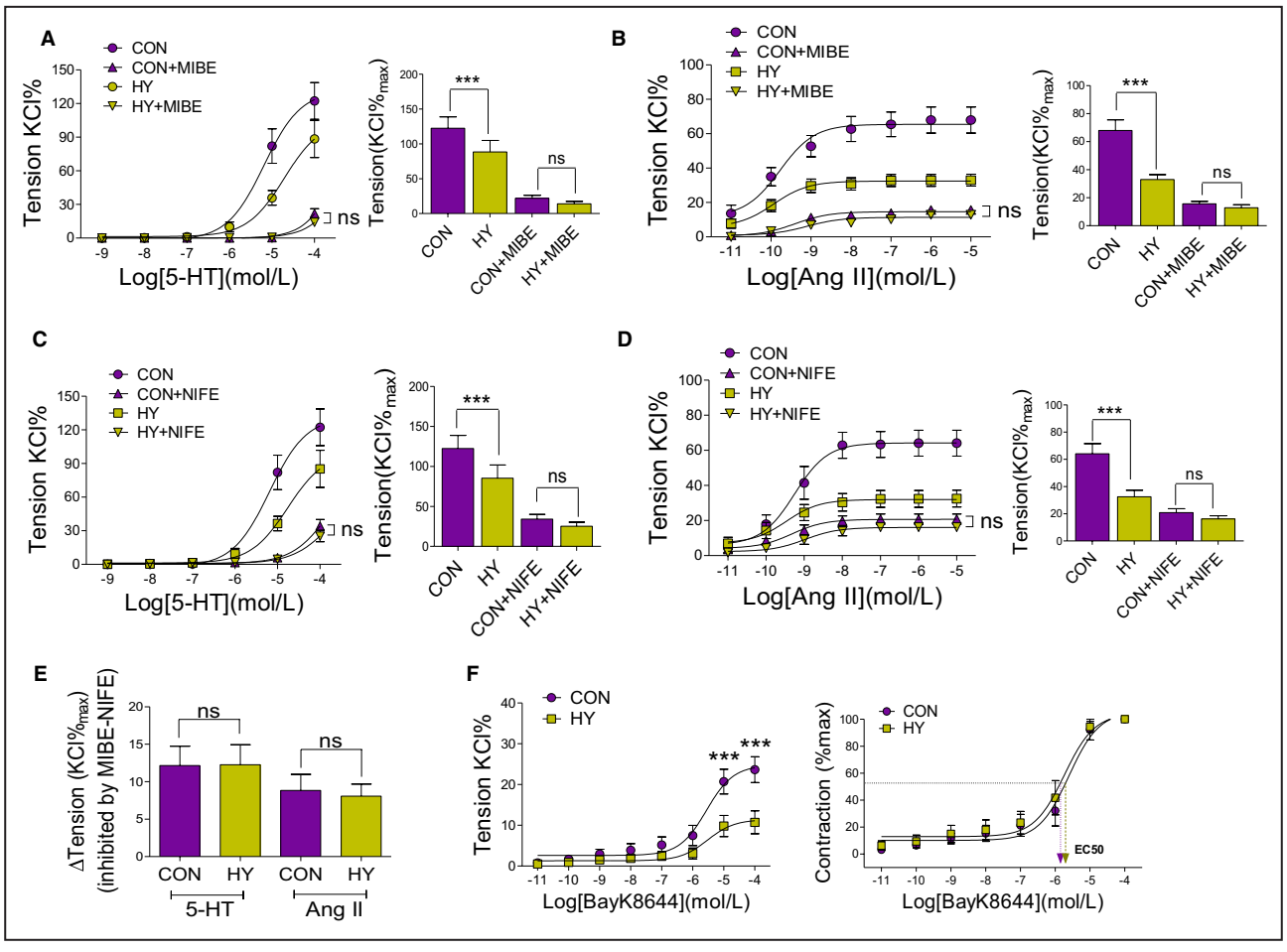

Figure 3. Antenatal hypoxia-decreased vascular contractility was correlated with L-type Ca^{2+} channels (LTCCs).
A and **B**, Serotonin hydrochloride (5-HT) or angiotensin Ang II-induced contractions in the presence or absence of mibefradil (MIBE; antagonist for L- and T-type calcium channels) in offspring PA rings (N=5, n=10). **C** and **D**, 5-HT or angiotensin II (Ang II)-induced contractions in the presence or absence of nifedipine (NIFE; antagonist for LTCCs) in offspring PA rings (N=5, n=10). **E**, △Tension (inhibited by MIBE-NIFE) on 5-HT or angiotensin II–induced maximal contractions) (N=5, n=10). **F**, BayK8644-induced vasoconstrictions and EC_{50} in offspring PA rings (N=5, n=10). Data were presented as means±SEM. N, number of adult male offspring from different litters of each group; n, number of PA rings. Data were analyzed by Student *t* test or 2-way ANOVA followed by Bonferroni posttests. ***P<0.001. CON indicates control group; HY, hypoxia group; and ns, nonsignificance.

Ca^{2+} Transients in Offspring PA Myocytes

LTCCs have been shown to be dominant in vascular myocyte constriction. To determine changes of LTCCs in antenatal hypoxic PA myocytes, representative traces of Ca^{2+} transients elicited by BayK8644 were measured with the fluorescence Ca^{2+} indicator Fluo-3 AM using the advanced Ca^{2+} imaging techniques (total internal reflection fluorescence microscopy electron-multiplying charge-coupled device imaging system). As shown in Figure 4, BayK8644 (Figure 4A through 4C), 5-HT– (Figure 4D and 4E) or angiotensin II (Figure 4G through 4I)-induced Ca^{2+} transients were lower in antenatal hypoxic PA myocytes with lower value of area under the curve and maximum fluorescence ratio (F/F0). Nifedipine could significantly inhibit 5-HT– or angiotensin II–mediated Ca^{2+} transients in both groups (Figure 4D through 4I). After pretreatment with nifedipine, no significant differences were observed in 5-HT– or angiotensin II–mediated Ca^{2+} transients between the 2 groups (Figure 4D through 4I). These data together indicated that antenatal hypoxia decreased agonist-mediated Ca^{2+} transients and were correlated to LTCCs in the offspring PA myocytes.

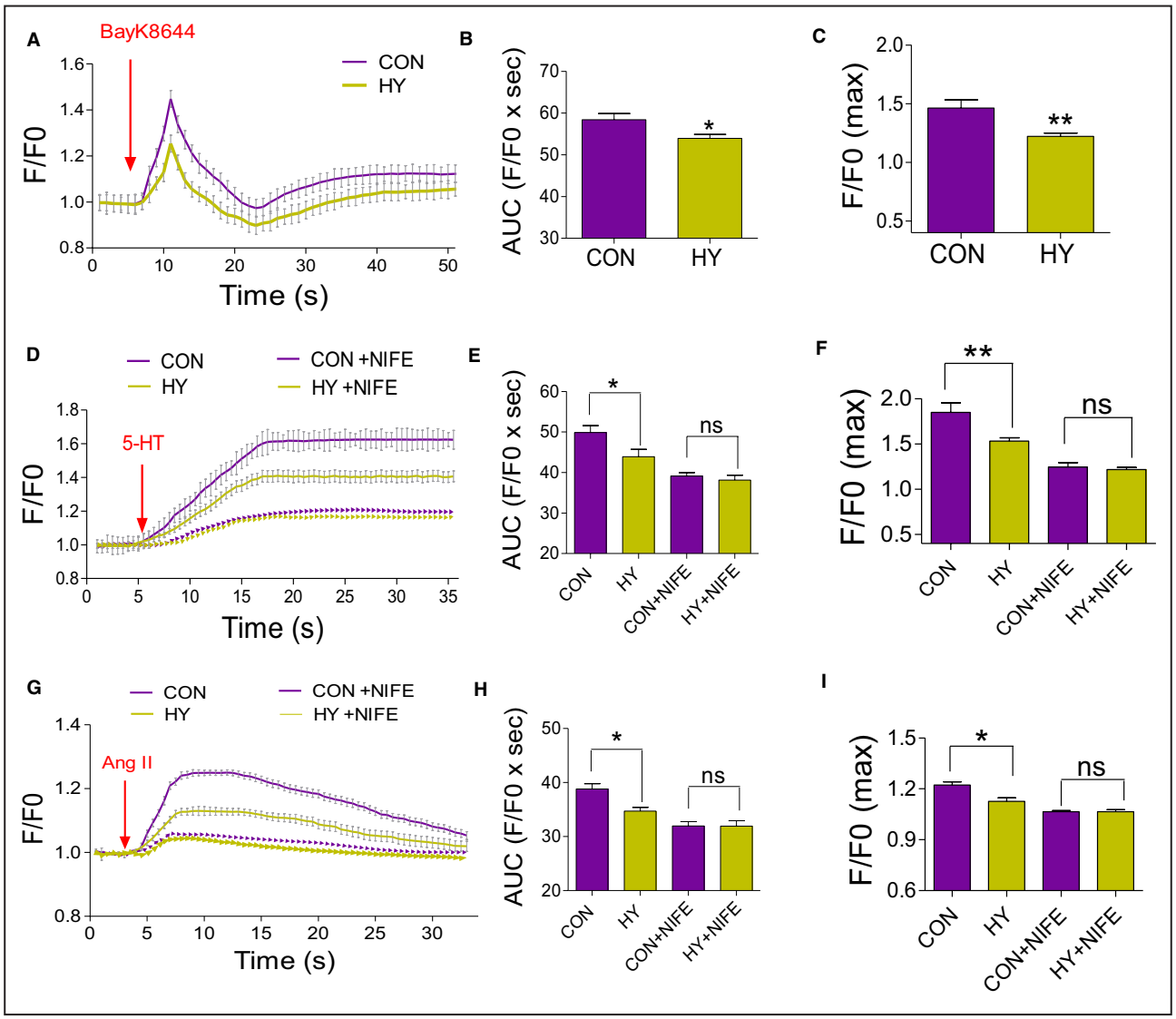

Figure 4. Ca^{2+} transients in offspring pulmonary artery (PA) myocytes.
A through **C**, BayK8644-induced Ca^{2+} increases in single isolated myocyte. Representative traces (**A**) and statistics of Ca^{2+} transients elicited by BayK8644 measured with the fluorescence Ca^{2+} indicator Fluo-3 AM. Area under the curve (**B**), and maximum of Ca^{2+} responses (**C**) was calculated. The fractional fluorescence intensity was calculated as F/F0, where F is the fluorescence intensity for the region of interest, and F0 is the fluorescence intensity during a period from the beginning of the recording when there was no Ca^{2+} activity (n=30 cells from 6 rats per group). **D** through **I**, Serotonin hydrochloride (5-HT) (**D** through **F**) or angiotensin II (Ang II) (**G** through **I**)-induced Ca^{2+} increases in the presence or absence of NIFE (n=20 cells from 6 rats per group). Data were presented as means±SEM. n, number of PA myocytes. Data were analyzed by Student *t* test. **P*<0.05; ***P*<0.01. CON indicates control group; HY, hypoxia group; and ns, nonsignificance.

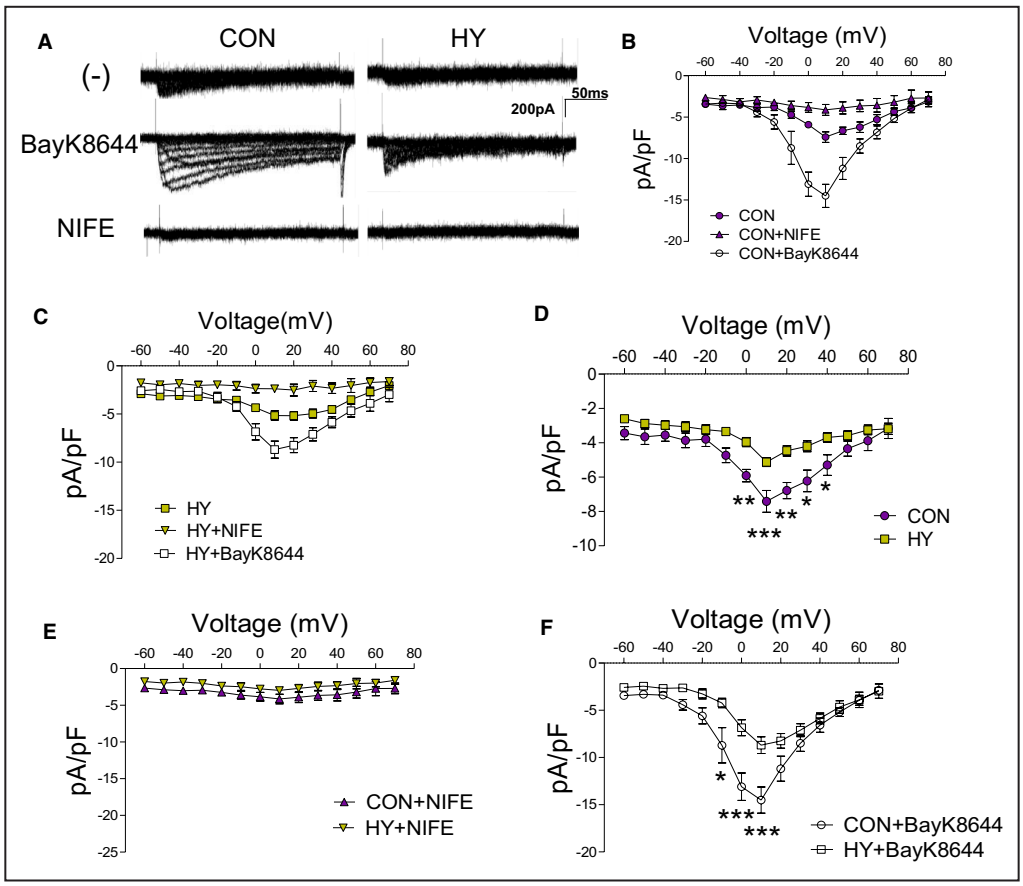

Figure 5. L-type Ca^{2+} channels (LTCCs) in offspring pulmonary artery (PA) myocytes.
A, Representative traces of Ca^{2+} currents evoked by command potentials (–60 to +70 mV, in 10-mV step) in the absence (upper, [–]) or presence of BayK8644 (center) or nifedipine (lower, nifedipine [NIFE]). **B** and **C**, Mean current density-voltage relationships of Ca^{2+} currents in the control (**B**) and hypoxia (**C**) group (N=5, n=20 cells for each group). **D** through **F**, Mean current density-voltage relationships of Ca^{2+} currents in the absence (**D**) or presence of nifedipine (**E**) or BayK8644 (**F**) between the 2 groups (N=5, n=20 cells for each group). Data were presented as means±SEM. N, number of adult male offspring from different litters of each group; n, number of PA myocytes. Data were analyzed by 2-way ANOVA followed by Bonferroni posttests. **P*<0.05; ***P*<0.01; ****P*<0.001. CON indicates control group; and HY, hypoxia group.

LTCCs in Offspring PA Myocytes

To determine possible changes of LTCCs in antenatal hypoxic PA myocytes, whole-cell LTCC currents were recorded with a conventional whole-cell patch clamp. The Ca^{2+} currents were evoked by command potentials (–60 to +70 mV in a 10-mV step) in the absence (upper, [–]) or presence of BayK8644 (center) or nifedipine (lower) (Figure 5A). In both groups, BayK8644 increased the peak inward current of Ca^{2+} currents, whereas nifedipine almost completely inhibited the Ca^{2+} currents (Figure 5B and 5C). In Figure 5D, the real-time recordings showed that amplitude of Ca^{2+} currents was lower in the hypoxia group from 0 to +40 mV. After pretreatment with nifedipine, no significant differences were observed in current density-voltage relationships between the 2 groups (Figure 5E). Meanwhile, BayK8644-increased Ca^{2+} currents were lower in hypoxia group from –10 to +10 mV (Figure 5F). These data together indicated that antenatal hypoxia impaired LTCCs in the offspring PA myocytes.

Expressions of LTCCs in the Offspring PA

In vascular smooth muscle cells, membrane depolarization activates LTCCs and alters the electrochemical gradient acting on sodium–calcium exchanger, which shifts the latter into a "reverse mode," providing for additional extracellular Ca^{2+} entry. Furthermore, the receptor-coupling processes can also activate nonselective cation channels, allowing for extracellular Ca^{2+} entry. Reports also show that sodium–calcium exchanger and transient receptor potential channels, which encode for nonselective cation channels, contribute to the development of PA hypertension.[32] Therefore, the effect of antenatal hypoxia on these Ca^{2+} channels are worth exploring. As shown in Figure S5A and S5B, antenatal hypoxia did not alter

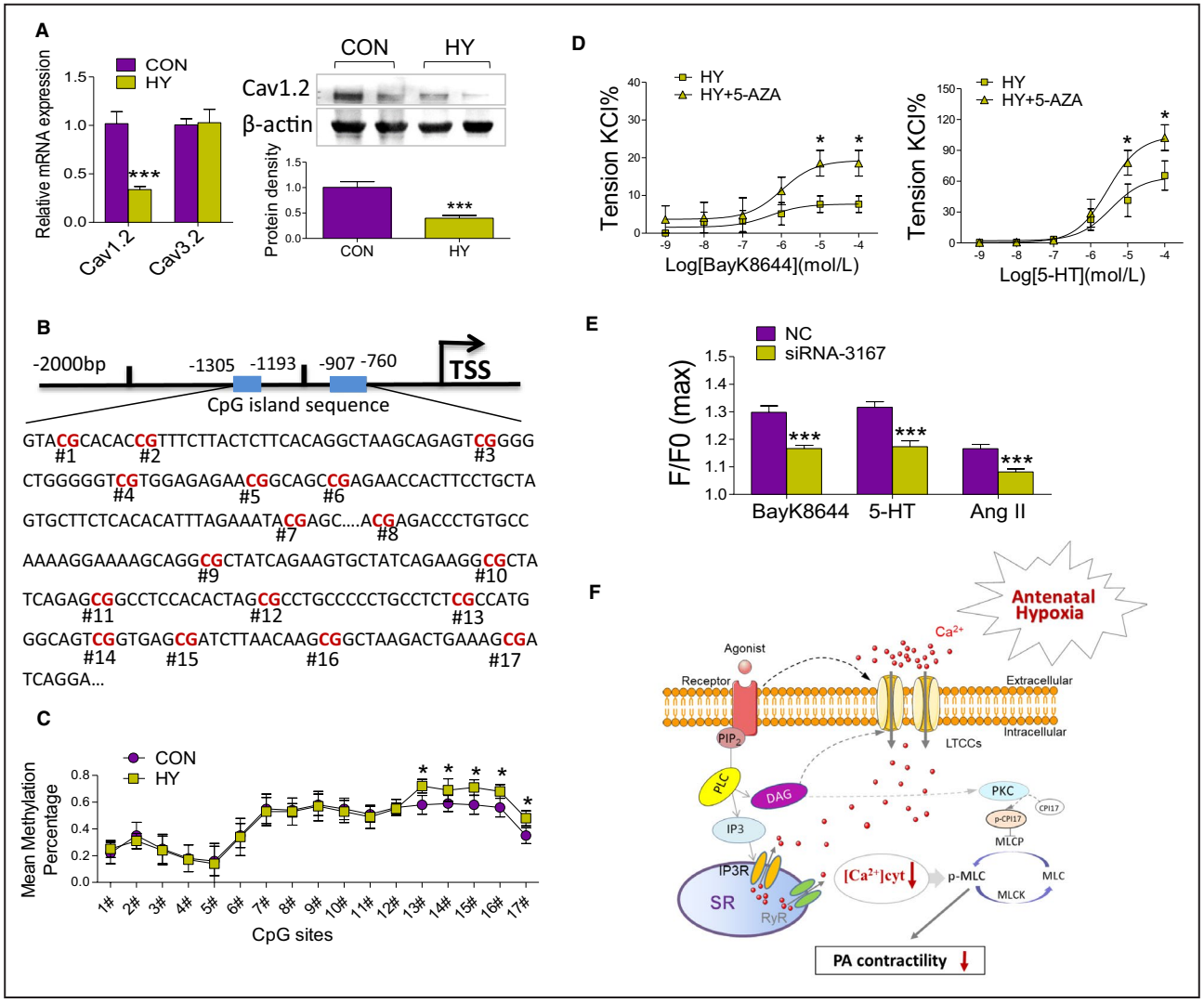

Figure 6. Expressions of L-type Ca^{2+} channels (LTCCs) in offspring pulmonary arteries (PAs).
A, mRNA and protein levels of Cav1.2, and (or) Cav3.2 in adult offspring PAs determined by quantitative real-time polymerase chain reaction and Western blot (N=10 for each group). **B**, Bioinformatic analysis of CpG islands of *Cav1.2* from upstream −2 kb to downstream +2 kb region. Sequence analysis identified two CpG islands that contain 17 CpG sites, located at positions −1305 to −1193, −907 to −760 from the translation start site (defined as position 1) in *Cav1.2* gene promoter. **C**, The mean methylation status of each tested CpG site in the adult offspring PAs (N=20 each group). **D**, BayK8644 (left) or serotonin hydrochloride (5-HT; right)-induced contractions in offspring PA rings after treatment with 5-AZA-2'-deoxycytidine (DNA methyltransferase inhibitor) (N=3, n=8). **E**, BayK8644 or 5-HT-induced Ca^{2+} transients in control offspring PA myocytes after knockdown Cav1.2 (N=3, n=20 cells for each group). **F**, Summarized image of the mechanism of vascular hypo-contractility in antenatal hypoxia offspring PAs. Data were presented as means±SEM. N, number of adult male offspring, n, number of PA rings or myocytes. Data were analyzed by Student *t* test or two-way ANOVA followed by Bonferroni post-tests. **P*<0.05; ****P*<0.001. CPI17 indicates protein phosphatase 1 regulatory inhibitor; DAG, diacylglycerol; IP3, inositol 1,4,5-trisphosphate; IP3R, IP3 receptor; MLC, myosin light chain; MLCK, MLC kinase; MLCP, MLC phosphatase; p-CPI17, phosphorylated CPI17; PIP2, phosphatidylinositol 4,5- bisphosphate; PKC, protein kinase C; PLC, phospholipase C; p-MLC, phosphorylated MLC; RYR, ryanodine receptors; and SR, sarcoplasmic reticulum.

the expressions of sodium–calcium exchanger 1-3 and transient receptor potential channels 1-7 in the offspring PA. Cav1.2 and alpha1 H (Cav3.2) are the main source of Ca^{2+} influx in most vascular myocytes. Figure 6A showed that expression levels of Cav1.2, not L-type Ca^{2+} channel subunit alpha1 H were decreased in the hypoxia group. Sequence analysis identified 2 CpG islands that contain 17 CpG sites within the *Cav1.2* gene promoter (Figure 6B). Bisulfite sequencing showed that methylation levels of these CpG sites in antenatal hypoxia PA were increased with specific CpG sites (13–17) (Figure 6C). We also assessed the effects of inhibiting DNA methylation on PA vasoreactivity. In adult offspring PA, 5-AZA treatment significantly increased the sensitivity to BayK8644 and 5-HT (Figure 6D, Figure S5C). Next,

we sought to determine the direct relation between Cav1.2 expression and Ca^{2+} transients. We designed and validated the efficacy and specificity of siRNAs against Cav1.2 (Figure S5D). Transfected PA myocytes with negative control siRNA, siRNA-3167, respectively, and analyzed Ca^{2+} transients induced by vascular agonists. Results confirmed that Cav1.2-knockdown significantly decreased BayK8644 or 5-HT–mediated Ca^{2+} transients (Figure 6E).

DISCUSSION

Hypoxia is a signal guiding placental development. Once hemochorial placentation is established, higher intrauterine oxygen levels are indispensable for placental function and fetal development. Consequently, hypoxia in utero usually occurs in middle and late pregnancy. This study used rat models to mimic clinical intrauterine fetal hypoxia in mid-late pregnancy, to reveal the effects of hypoxia on PA vascular function and clarify its underlying mechanisms. The data gained in this study suggest that hypoxia during pregnancy disrupted the contractile mechanism of PA myocytes, manifested in the process of impaired Ca^{2+} inflow during contraction. The major novel findings are as follows: (1) PA contraction was decreased in response to 5-HT, angiotensin II, or phenylephrine in antenatal hypoxic offspring. (2) Such vascular insensitivity was associated with LTCCs. The baseline and agonist-induced LTCC currents were decreased in antenatal hypoxic offspring PA myocytes. (3) Antenatal hypoxic offspring PA exhibited reduced Cav1.2 expression, increased promoter methylations within *Cav1.2*. Together, this study provides direct evidence showing that antenatal hypoxia-reprogrammed *Cav1.2* gene expression patterns could be associated with DNA methylation status, led to perturbed Ca^{2+} signaling in PA myocytes, resulting in long-term vascular hypocontractility outcomes in adult offspring. Figure 6F summarized the working model.

PAs are very sensitive to hypoxia. Long-term hypoxia, such as occurs at high altitude, can lead to a number of problems in PA vascular reactivities.[33,34] Keegan et al[34] indicated that long-term hypoxia enhances 5-HT–induced PA contraction via Ca^{2+} signaling in rats and mice. Wan[35] and colleagues demonstrated that chronic hypoxia selectively enhances LTCC activity in the PA by upregulating Cav1.2 and L-type Ca^{2+} channel subunit alpha1 H. In addition, recent studies suggest that hypoxia during gestation altered neonatal PA vascular reactivity as a consequence of changes in extracellular Ca^{2+} entry.[36,37] For example, prenatal hypoxia can increase 5-HT–mediated PA contraction and associated extracellular Ca^{2+} influx through LTCCs in the near-term fetus.[37] All those studies indicated that hypoxia occurred perinatally or postnatally and could affect PA vascular reactivity via altering extracellular Ca^{2+} entry by LTCCs.[37,38] Antenatal stress can lead to vascular dysfunction in the fetus and is a risk factor for the development of persistent vascular dysfunction in the offspring.[1,2] Although it is well established that antenatal hypoxia alters PA vascular reactivities and Ca^{2+} signaling in the developing fetus, it is unknown whether antenatal hypoxia also can alter PA reactivities and underlying Ca^{2+} signaling processes in the mature animals. Thus, we tested the hypothesis that antenatal hypoxia may alter PA contraction and associated extracellular Ca^{2+} influx through LTCCs in the adult offspring.

Cav1.2 is likely vulnerable and sensitive to antenatal insults.[20,21] For example, antenatal insults could impair vascular functions by altering Cav1.2 expression in the offspring small arteries.[20,21] Maternal high-sucrose diet accelerated vascular stiffness and hypocontractility via suppressing Cav1.2 in the offspring mesenteric arteries.[20] Whole-cell current density and expression of Cav1.2 were decreased in mesenteric artery myocytes from the salt-loading offspring rats exposed to prenatal hypoxia.[21] Prenatal stress also altered the expressions or functions of Cav1.2 in other tissue of offspring, such as the hippocampus[39,40] and pancreas islet.[41] As one of the most common pathological processes for the developmental fetus, hypoxia in utero can impair vascular functions in offspring.[42,43] Recently, we discovered that antenatal hypoxia could induce vascular dysfunction in the small arteries of adult offspring.[9,44] Antenatal hypoxic offspring cerebral arteries[9] and renal interlobar arteries[44] exhibited agonist-induced vascular hypercontractility along with increasing Cav1.2 expression. These strongly suggested that the effects of different maternal stressors on Cav1.2 expression and activity in the vasculature could be different. Interestingly, this study observed the opposite effect of antenatal hypoxia on offspring PA. Antenatal hypoxic offspring PA exhibited agonist-induced vascular hypocontractility accompanied by decreasing Cav1.2 expression. This is the first report to imply that there was a vessel tissue–dependent property of the effect of antenatal hypoxia on offspring vascular Cav1.2.

In the present study, Cav1.2 mRNA levels were decreased, indicating that its expression was regulated through a transcriptional mechanism. Epigenetic modifications related to relatively stable and heritable patterns of gene expression, which mainly are mediated by DNA methylation, have been indicated to play crucial roles in developmental origins of vascular diseases.[2] Key developmental stages are defined

by dramatic DNA methylation changes that may be susceptible/responsive to environmental cues. Gene expression could be enhanced through a decrease in DNA methylation of its promoter CpG islands. To investigate possible epigenetic dysregulation of the *Cav1.2* gene, we evaluated the methylation status of its promoter and found that the methylation levels of CpG sites within *Cav1.2* gene were increased with specific CpG sites (13–17) in the antenatal hypoxia group. The increased promoter methylations within *Cav1.2* were compatible with its reduced expression. Next, to clarify whether the inactivated transcription of Cav1.2 is attributable to promoter methylation alterations, we assessed changes of Cav1.2 transcription after adding 5-AZA in antenatal hypoxia offspring PA rings. 5-AZA treatment significantly increased Cav1.2 expression and the sensitivity to vascular agonist in PA rings. Taken together, our results indicated there was a correlation between DNA methylation, Cav1.2 expression, and vascular contractility, and suggested that antenatal hypoxia decreased PA contractility in offspring, which was potentially associated with inactivated transcription of Cav1.2 by reprogramming DNA methylation patterns.

Pulmonary hypertension is a heterogeneous clinical syndrome with a poor prognosis, which involves vasoconstriction and progressive structural remodeling of the PA, resulting in right ventricular hypertrophy and failure. A hallmark of pulmonary hypertension in newborns as well as adults is that the contractility of PA is dysregulated.[12,13] Under pathophysiological conditions, PA hypercontractility led to enhanced PA vascular resistance and subsequent pulmonary hypertension.[12,13] The arterial contraction is mainly initiated by cytosolic Ca^{2+} increases within myocytes that line the vessel wall. LTCCs are well known as central to the rise in cytosolic Ca^{2+} and resultant arterial contractions. Dysregulation of LTCC expressions and functions is important to the development of pulmonary hypertension and other vascular diseases.[14,15] Human and animal data have shown that hypoxia in the fetus and/or newborn was associated with an increased risk of pulmonary hypertension.[45] It is well known that chronic intrauterine hypoxia fetus usually exhibited an enhanced PA contractility and associated extracellular Ca^{2+} influx through LTCCs in the near-term fetus.[37] However, the present study indicated that adult offspring with antenatal hypoxia exhibited PA hypo induced by vascular agonists contractility and decreased Cav1.2. There may be various reasons for this discrepancy. One major cause may be a compensatory effect: The downregulation of Cav1.2 was highly likely to be compensatory protection for the antenatal hypoxia-induced PA hypercontractility in the fetus. Fetal lungs are not fully developed until after birth. It is more plausible that the observed downregulated Cav1.2 in the postnatal stage represents an adaptive readjustment in response to the hypoxia-damaged LTCCs at the fetal stage. In addition, after 2 weeks of hypoxia, antenatal hypoxic offspring PA still exhibited lower agonist-induced contractions than that in control offspring (Figure S6). These data indicated that PA contractility of antenatal hypoxic offspring was insensitive to hypoxia again after birth and implied that Cav1.2 compensatory downregulation may protect antenatal hypoxic offspring with hypoxia again.

In summary, the data in this study indicate that antenatal hypoxia disrupted the contractile mechanism of PA, manifested in the process of impairing Ca^{2+} inflow via LTCCs during contraction. Our findings are important, as they offer new information about pathological characteristics of PA in antenatal hypoxic adult offspring. Nevertheless, there are some limitations to this study. For example, we examined only male offspring. For a deeper understanding of the role of antenatal hypoxia, future work should also examine female offspring. To fully elucidate the long-term effects, studies should also be conducted in different developing ages and even in the next generation. Additionally, antenatal hypoxia is a common intrauterine stress for the developing fetus. The PA is sensitive to antenatal hypoxia, and such a side effect would persist into adulthood. Hence, further clinical observation of the individuals who had antenatal hypoxia are necessary to verify our study results.

ARTICLE INFORMATION

Received October 25, 2020; accepted March 4, 2021.

Affiliation

From the Institute for Fetology, First Hospital of Soochow University, Suzhou, China.

Acknowledgments

We thank Tian Hao Biotechnology Co., Ltd., Shanghai, China for the excellent technical assistance.

Author contributions: Drs Gao and Z. Xu conceived and designed experiments and wrote the manuscript. Drs Gao, Li, Ji, T. Xu, and Zhao performed most of the experiments, analyzed the data, and prepared figures. All authors reviewed and gave approval of the final draft.

Sources of Funding

This work was supported partly by the Ministry of Science and Technology of China (2019YFA0802600), National Nature & Science Foundation of China (81873841, 81741024, and 81401244), "333 Project," "Six one project (LGY2018076)," and the Suzhou city "Wei Sheng Ren Cai (GSWS2019029)" program.

Disclosures

None.

Supplementary Material

Tables S1–S2
Figures S1–S6

REFERENCES

1. Walker A, Walker BF, Dobbing J. Fetal nutrition and cardiovascular disease in adult life. *Lancet*. 1993;341:1421. DOI: 10.1016/0140-6736(93)90995-S.

2. Gao Q, Tang J, Chen J, Jiang L, Zhu X, Xu Z. Epigenetic code and potential epigenetic-based therapies against chronic diseases in developmental origins. *Drug Discov Today*. 2014;19:1744–1750. DOI: 10.1016/j.drudis.2014.05.004.
3. Fryer BH, Simon MC. Hypoxia, HIF and the placenta. *Cell Cycle*. 2006;5:495–498. DOI: 10.4161/cc.5.5.2497.
4. Dunwoodie SL. The role of hypoxia in development of the mammalian embryo. *Dev Cell*. 2009;17:755–773. DOI: 10.1016/j.devcel.2009.11.008.
5. Jauniaux E, Watson A, Burton G. Evaluation of respiratory gases and acid-base gradients in human fetal fluids and uteroplacental tissue between 7 and 16 weeks' gestation. *Am J Obstet Gynecol*. 2001;184:998–1003. DOI: 10.1067/mob.2001.111935.
6. Ducsay CA, Goyal R, Pearce WJ, Wilson S, Hu XQ, Zhang L. Gestational hypoxia and developmental plasticity. *Physiol Rev*. 2018;98:1241–1334. DOI: 10.1152/physrev.00043.2017.
7. Mandruzzato G, Antsaklis A, Botet F, Chervenak FA, Figueras F, Grunebaum A, Puerto B, Skupski D, Stanojevic M; WAPM. Intrauterine restriction (IUGR). *J Perinat Med*. 2008;36:277–281. DOI: 10.1515/JPM.2008.050.
8. Liu B, Liu Y, Shi R, Feng X, Li X, Zhang W, Wu J, Li N, Zhou X, Sun M, et al. Chronic prenatal hypoxia down-regulated BK channel Beta1 subunits in mesenteric artery smooth muscle cells of the offspring. *Cell Physiol Biochem*. 2018;45:1603–1616. DOI: 10.1159/000487727.
9. Tang J, Li N, Chen X, Gao Q, Zhou X, Zhang Y, Liu B, Sun M, Xu Z. Prenatal hypoxia induced dysfunction in cerebral arteries of offspring rats. *J Am Heart Assoc*. 2017;6:e006630. DOI: 10.1161/JAHA.117.006630.
10. Chen X, Qi L, Su H, He Y, Li N, Gao Q, Li H, Xu T, Lu L, Xu Z, et al. Prenatal hypoxia attenuated contraction of offspring coronary artery associated with decreased PKCbeta Ser(660) phosphorylation and intracellular calcium. *Life Sci*. 2020;261:118364. DOI: 10.1016/j.lfs.2020.118364.
11. Zhu X, Gao Q, Tu Q, Zhong Y, Zhu D, Mao C, Xu Z. Prenatal hypoxia enhanced angiotensin II-mediated vasoconstriction via increased oxidative signaling in fetal rats. *Reprod Toxicol*. 2016;60:21–28. DOI: 10.1016/j.reprotox.2016.01.001.
12. Di Salvo TG. Pulmonary hypertension and right ventricular failure in left ventricular systolic dysfunction. *Curr Opin Cardiol*. 2012;27:262–272. DOI: 10.1097/HCO.0b013e3283522098.
13. Bonnet S, Archer SL. Potassium channel diversity in the pulmonary arteries and pulmonary veins: implications for regulation of the pulmonary vasculature in health and during pulmonary hypertension. *Pharmacol Ther*. 2007;115:56–69. DOI: 10.1016/j.pharmthera.2007.03.014.
14. Wang J, Weigand L, Foxson J, Shimoda LA, Sylvester JT. Ca^{2+} signaling in hypoxic pulmonary vasoconstriction: effects of myosin light chain and Rho kinase antagonists. *Am J Physiol Lung Cell Mol Physiol*. 2007;293:L674–L685. DOI: 10.1152/ajplung.00141.2007.
15. Pourmahram GE, Snetkov VA, Shaifta Y, Drndarski S, Knock GA, Aaronson PI, Ward JP. Constriction of pulmonary artery by peroxide: role of Ca^{2+} release and PKC. *Free Radic Biol Med*. 2008;45:1468–1476. DOI: 10.1016/j.freeradbiomed.2008.08.020.
16. Berridge MJ. The inositol trisphosphate/calcium signaling pathway in health and disease. *Physiol Rev*. 2016;96:1261–1296. DOI: 10.1152/physrev.00006.2016.
17. Urena J, del Valle-Rodriguez A, Lopez-Barneo J. Metabotropic Ca^{2+} channel-induced calcium release in vascular smooth muscle. *Cell Calcium*. 2007;42:513–520. DOI: 10.1016/j.ceca.2007.04.010.
18. Eid AH, El-Yazbi AF, Zouein F, Arredouani A, Ouhtit A, Rahman MM, Zayed H, Pintus G, Abou-Saleh H. Inositol 1,4,5-trisphosphate receptors in hypertension. *Front Physiol*. 2018;9:1018.: DOI: 10.3389/fphys.2018.01018.
19. Navedo MF, Cheng EP, Yuan C, Votaw S, Molkentin JD, Scott JD, Santana LF. Increased coupled gating of L-type Ca^{2+} channels during hypertension and Timothy syndrome. *Circ Res*. 2010;106:748–756. DOI: 10.1161/CIRCRESAHA.109.213363.
20. Feng X, Li X, Yang C, Ren Q, Zhang W, Li N, Zhang M, Zhang B, Zhang L, Zhou X, et al. Maternal high-sucrose diet accelerates vascular stiffness in aged offspring via suppressing Cav 1.2 and contractile phenotype of vascular smooth muscle cells. *Mol Nutr Food Res*. 2019;63:e1900022. DOI: 10.1002/mnfr.201900022.
21. Liu B, Shi R, Li X, Liu Y, Feng X, Chen X, Fan X, Zhang Y, Zhang W, Tang J, et al. Downregulation of L-type voltage-gated Ca(2+), voltage-gated K(+), and large-conductance Ca(2+)-activated K(+) channels in vascular myocytes from salt-loading offspring rats exposed to prenatal hypoxia. *J Am Heart Assoc*. 2018;7:e008148. DOI: 10.1161/JAHA.117.008148.
22. Mu YP, Lin DC, Zheng SY, Jiao HX, Sham JSK, Lin MJ. Transient receptor potential melastatin-8 activation induces relaxation of pulmonary artery by inhibition of store-operated calcium entry in normoxic and chronic hypoxic pulmonary hypertensive rats. *J Pharmacol Exp Ther*. 2018;365:544–555. DOI: 10.1124/jpet.117.247320.
23. Li X, Feng X, Lu L, He A, Liu B, Zhang Y, Shi R, Liu Y, Chen X, Sun M, et al. Prenatal hypoxia plus postnatal high-fat diet exacerbated vascular dysfunction via up-regulated vascular Cav1.2 channels in offspring rats. *J Cell Mol Med*. 2019;23:1183–1196. DOI: 10.1111/jcmm.14020.
24. Li N, Li Y, Gao Q, Li D, Tang J, Sun M, Zhang P, Liu B, Mao C, Xu Z. Chronic fetal exposure to caffeine altered resistance vessel functions via RyRs-BKCa down-regulation in rat offspring. *Sci Rep*. 2015;5:13225. DOI: 10.1038/srep13225.
25. Gao Q, Li H, Ding H, Fan X, Xu T, Tang J, Liu Y, Chen X, Zhou X, Tao J, et al. Hyper-methylation of AVPR1A and PKCBeta gene associated with insensitivity to arginine vasopressin in human pre-eclamptic placental vasculature. *EBioMedicine*. 2019;44:574–581. DOI: 10.1016/j.ebiom.2019.05.056.
26. Xu T, Zhao M, Li H, Zhou X, Liu B, Sun M, Xu Z, Gao Q. Antenatal dexamethasone exposure impairs the high-conductance Ca(2+)-activated K(+) channels via epigenetic alteration at gene promoter in male offspring. *Arterioscler Thromb Vasc Biol*. 2020;40:e284–e295. DOI: 10.1161/ATVBAHA.120.314905.
27. Wynne BM, Chiao CW, Webb RC. Vascular smooth muscle cell signaling mechanisms for contraction to angiotensin II and endothelin-1. *J Am Soc Hypertens*. 2009;3:84–95. DOI: 10.1016/j.jash.2008.09.002.
28. Foskett JK, White C, Cheung KH, Mak DO. Inositol trisphosphate receptor Ca^{2+} release channels. *Physiol Rev*. 2007;87:593–658. DOI: 10.1152/physrev.00035.2006.
29. Song J, Eyster KM, Kost CK Jr, Kjellsen B, Martin DS. Involvement of protein kinase C-CPI-17 in androgen modulation of angiotensin II-renal vasoconstriction. *Cardiovasc Res*. 2010;85:614–621. DOI: 10.1093/cvr/cvp326.
30. Ringvold HC, Khalil RA. Protein kinase C as regulator of vascular smooth muscle function and potential target in vascular disorders. *Adv Pharmacol*. 2017;78:203–301. DOI: 10.1016/bs.apha.2016.06.002.
31. Tong L, Ao JP, Lu HL, Huang X, Zang JY, Liu SH, Song NN, Huang SQ, Lu C, Chen J, et al. Tyrosine kinase Pyk2 is involved in colonic smooth muscle contraction via the RhoA/ROCK pathway. *Physiol Res*. 2019;68:89–98. DOI: 10.33549/physiolres.933857.
32. Yu Y, Fantozzi I, Remillard CV, Landsberg JW, Kunichika N, Platoshyn O, Tigno DD, Thistlethwaite PA, Rubin LJ, Yuan JX. Enhanced expression of transient receptor potential channels in idiopathic pulmonary arterial hypertension. *Proc Natl Acad Sci U S A*. 2004;101:13861–13866. DOI: 10.1073/pnas.0405908101.
33. Bonnet S, Belus A, Hyvelin JM, Roux E, Marthan R, Savineau JP. Effect of chronic hypoxia on agonist-induced tone and calcium signaling in rat pulmonary artery. *Am J Physiol Lung Cell Mol Physiol*. 2001;281:L193–L201. DOI: 10.1152/ajplung.2001.281.1.L193.
34. Keegan A, Morecroft I, Smillie D, Hicks MN, MacLean MR. Contribution of the 5-HT(1B) receptor to hypoxia-induced pulmonary hypertension: converging evidence using 5-HT(1B)-receptor knockout mice and the 5-HT(1B/1D)-receptor antagonist GR127935. *Circ Res*. 2001;89:1231–1239. DOI: 10.1161/hh2401.100426.
35. Wan J, Yamamura A, Zimnicka AM, Voiriot G, Smith KA, Tang H, Ayon RJ, Choudhury MS, Ko EA, Wang J, et al. Chronic hypoxia selectively enhances L- and T-type voltage-dependent Ca^{2+} channel activity in pulmonary artery by upregulating Cav1.2 and Cav3.2. *Am J Physiol Lung Cell Mol Physiol*. 2013;305:L154–L164. DOI: 10.1152/ajplung.00313.2012.
36. Xue Q, Ducsay CA, Longo LD, Zhang L. Effect of long-term high-altitude hypoxia on fetal pulmonary vascular contractility. *J Appl Physiol*. 2008;104:1786–1792. DOI: 10.1152/japplphysiol.01314.2007.
37. Goyal R, Papamatheakis DG, Loftin M, Vrancken K, Dawson AS, Osman NJ, Blood AB, Pearce WJ, Longo LD, Wilson SM. Long-term maternal hypoxia: the role of extracellular Ca^{2+} entry during serotonin-mediated contractility in fetal ovine pulmonary arteries. *Reprod Sci*. 2011;18:948–962. DOI: 10.1177/1933719111401660.
38. Shen CP, Romero M, Brunelle A, Wolfe C, Dobyns A, Francis M, Taylor MS, Puglisi JL, Longo LD, Zhang L, et al. Long-term high-altitude hypoxia influences pulmonary arterial L-type calcium channel-mediated Ca(2+) signals and contraction in fetal and adult sheep. *Am J Physiol Regul Integr Comp Physiol*. 2018;314:R433–R446. DOI: 10.1152/ajpregu.00154.2017.

39. Cai Q, Zhang B, Huang S, Wang T, Zhou T. The effects of prenatal stress on expression of CaMK-II and L-Ca^{2+} channel in offspring hippocampus. *Acta Biochim Biophys Sin*. 2011;43:601–606. DOI: 10.1093/abbs/gmr057.
40. Morton RA, Valenzuela CF. Further characterization of the effect of ethanol on voltage-gated Ca(2+) channel function in developing CA3 hippocampal pyramidal neurons. *Brain Res*. 2016;1633:19–26. DOI: 10.1016/j.brainres.2015.12.023.
41. Gatford KL, Mohammad SN, Harland ML, De Blasio MJ, Fowden AL, Robinson JS, Owens JA. Impaired beta-cell function and inadequate compensatory increases in beta-cell mass after intrauterine growth restriction in sheep. *Endocrinology*. 2008;149:5118–5127. DOI: 10.1210/en.2008-0233.
42. Hemmings DG, Williams SJ, Davidge ST. Increased myogenic tone in 7-month-old adult male but not female offspring from rat dams exposed to hypoxia during pregnancy. *Am J Physiol Heart Circ Physiol*. 2005;289:H674–H682. DOI: 10.1152/ajpheart.00191.2005.
43. Bourque SL, Gragasin FS, Quon AL, Mansour Y, Morton JS, Davidge ST. Prenatal hypoxia causes long-term alterations in vascular endothelin-1 function in aged male, but not female, offspring. *Hypertension*. 2013;62:753–758. DOI: 10.1161/HYPERTENSIONAHA.113.01516.
44. Tang J, Zhu Z, Xia S, Li NA, Chen N, Gao Q, Li L, Zhou X, Li D, Zhu X, et al. Chronic hypoxia in pregnancy affected vascular tone of renal interlobar arteries in the offspring. *Sci Rep*. 2015;5:9723. DOI: 10.1038/srep09723.
45. Papamatheakis DG, Blood AB, Kim JH, Wilson SM. Antenatal hypoxia and pulmonary vascular function and remodeling. *Curr Vasc Pharmacol*. 2013;11:616–640. DOI: 10.2174/1570161111311050006.

SUPPLEMENTAL MATERIAL

Table S1. The primers used in this study.

Primer/siRNA	Nucleotide Sequence (5’ to 3’)	
qRT-PCR primers	**Sense**	**Anti-sense**
Cav1.2	ACGTTACTGTGCGTTACATCTA	ATTAGCTTCTATGTCTGGTGTG
Cav3.2	CTACCTTATGACGACAACAATGC	GCATTGTAGACAGCAAGTACTT
NCX1	ACCCATGTTGACCATATAACTG	GCAATAATAGAAACTCCGAG
NCX2	GTGTGTCTATCATTGCTGATC	CCCTTAAGTGCTTGATCTTAC
NCX3	CAAGATTGCAAGGGTCATTGT	AGGTTGGAGACAGTTTCATTC
Stim1	TTTGGATTCTTCCCATTCTCAT	TCTCCTCACCAATAGAGCCAT
Orai1	TATCGTCTTTGCCGTTCACTT	GAAGGTGAGGACTTAGGCAT
ROCK1	GGACCATCTAGACAAGAAAGA	CAACATATCTCTTGCTGATGTT
ROCK2	TAGAGTGCCGTAGATGCCACAT	ATTTCTGCTGTTCTTCCGTTGA
RhoA	ATCTTCGGAATGATGAGCACA	GTTTGCCATATCTCTGCCTTCT
TRPC1	AGAGATGAGAACTACCAGAAG	AATCCCTTATTTCATTTCTGA
TRPC2	CCAGAAGGACCTGTATGAGATT	GAACTTCAGCAGGTCATATCGG
TRPC3	TCTCGCACGCTCAATGTC	AGAAGTCGTCATCGCGCA
TRPC4	AGCAAGCTCTCAACAATACAGT	AGAGGCTGAGATTCTTTCTCTT
TRPC5	TCCAAGCAGCAGCAGTAGG	TGTTCTCGCTCGGCTCTCT
TRPC6	GCGGAAGATGCTAGAAGAATGT	CTCCACAATCCGTACATAACCT
TRPC7	TCCTGCCTACATGTTCAATGAGA	AGTTCTCCTTCTTCAGCAGCAGT
Bisulfite sequencing PCR		
Cav1.2-BS1	GGAGYGTGTTTTAGGAGTTGGTATT	AAATCACACRTACTAAAAATAAACCTACAA
Cav1.2-BS2	GAAATAAYGAAGTTTGAGAGTTAAGAA	AACAATCACTAAAATCRAAACCAAAACTAC
siRNA		
Cav1.2-3167	GCCGAAAUUACUUCAAUAUTT	AUAUUGAAGUAAUUUCGGCTT
Cav1.2-4149	GGGUAGCAUUGUUGAUAUATT	UAUAUCAACAAUGCUACCCTT
Cav1.2-6414	GGGACAGUUUGCUCAAGAUTT	AUCUUGAGCAAACUGUCCCTT

Table S2. The effect of antenatal hypoxia on adult offspring (N=10) blood values.

Group / Index	Offspring (16 weeks old)	
	CON	HY
pH	7.36 ± 0.08	7.37 ± 0.07
pCO_2 (mmHg)	38.38 ± 1.64	39.77 ± 1.51
pO_2 (mmHg)	79.40 ± 3.28	79.29 ± 3.02
SO_2%	97.79 ± 1.01	98.37 ± 1.35
Hb (g/dl)	11.90 ± 0.81	12.03 ± 0.75
Hct (%)	42.68 ± 1.82	42.52± 1.92
Glucose (mmol/L)	7.75 ± 0.64	7.75 ± 0.46
Na^+ (mmol/L)	138.33 ± 1.79	137.86 ± 1.82
K^+ (mmol/L)	4.57 ± 0.26	4.58 ± 0.24
Osmolality (mOsm/Kg)	305.32 ± 2.91	305.62 ± 3.12

pH, potential of hydrogen; pO_2, partial pressure of oxygen; pCO_2, partial pressure of carbon dioxide; SO_2%, oxygen saturation; Hb, Hemoglobin; Hct, Hematocrit. Data are presented as the mean ± SEM. There were no statistical differences between the two groups. N means total number of adult offspring used.

Figure S1. A) Body weight of male offspring (N=15). B) Lung weight of male offspring (N=8). C) the representative images of hematoxylin and eosin (H&E) staining on pulmonary artery cross-sections of each group rats. D and E) are bar graphs showing wall thickness and pulmonary artery diameter in each group (N=5, n=10).

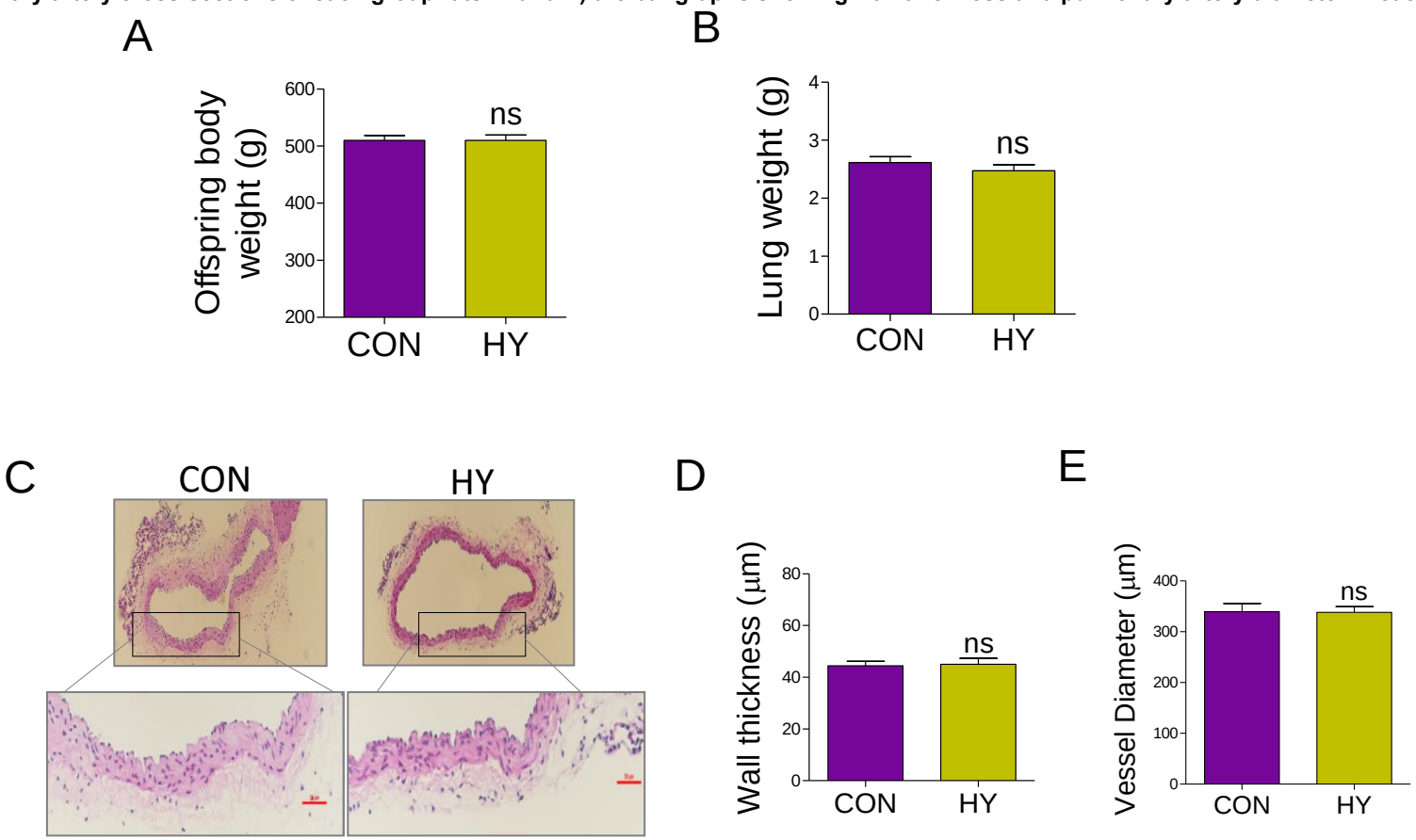

Data were presented as means ±SEM. N, number of male adult offspring from different litters of each group. n, number of pulmonary artery rings. Data were analyzed by Student's t test. ns, nonsignificance.

Figure S2. A and B) Phenylephrine-induced contraction and EC50 (concentration for 50% of maximal effect) in the offspring pulmonary artery rings (N=6, n = 12).

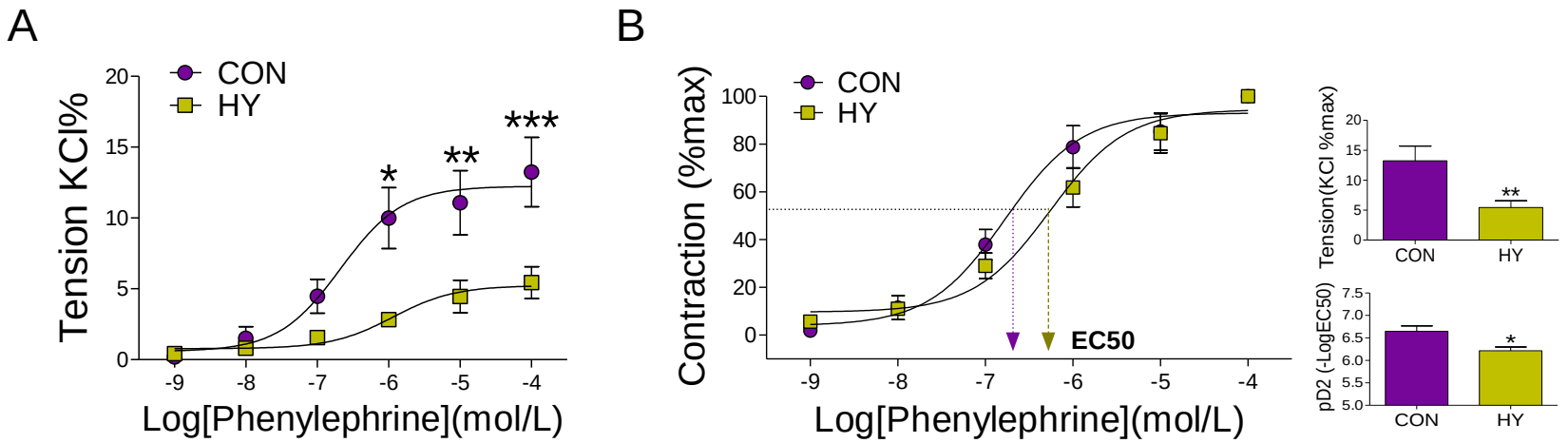

Data were presented as means ±SEM. N, number of male adult offspring from different litters of each group. n, number of pulmonary artery rings. Data were analyzed by Student's t test or two-way ANOVA followed by Bonferroni post-tests. *, $P < 0.05$; **, $P < 0.01$; ***, $P < 0.001$; ns, nonsignificance.

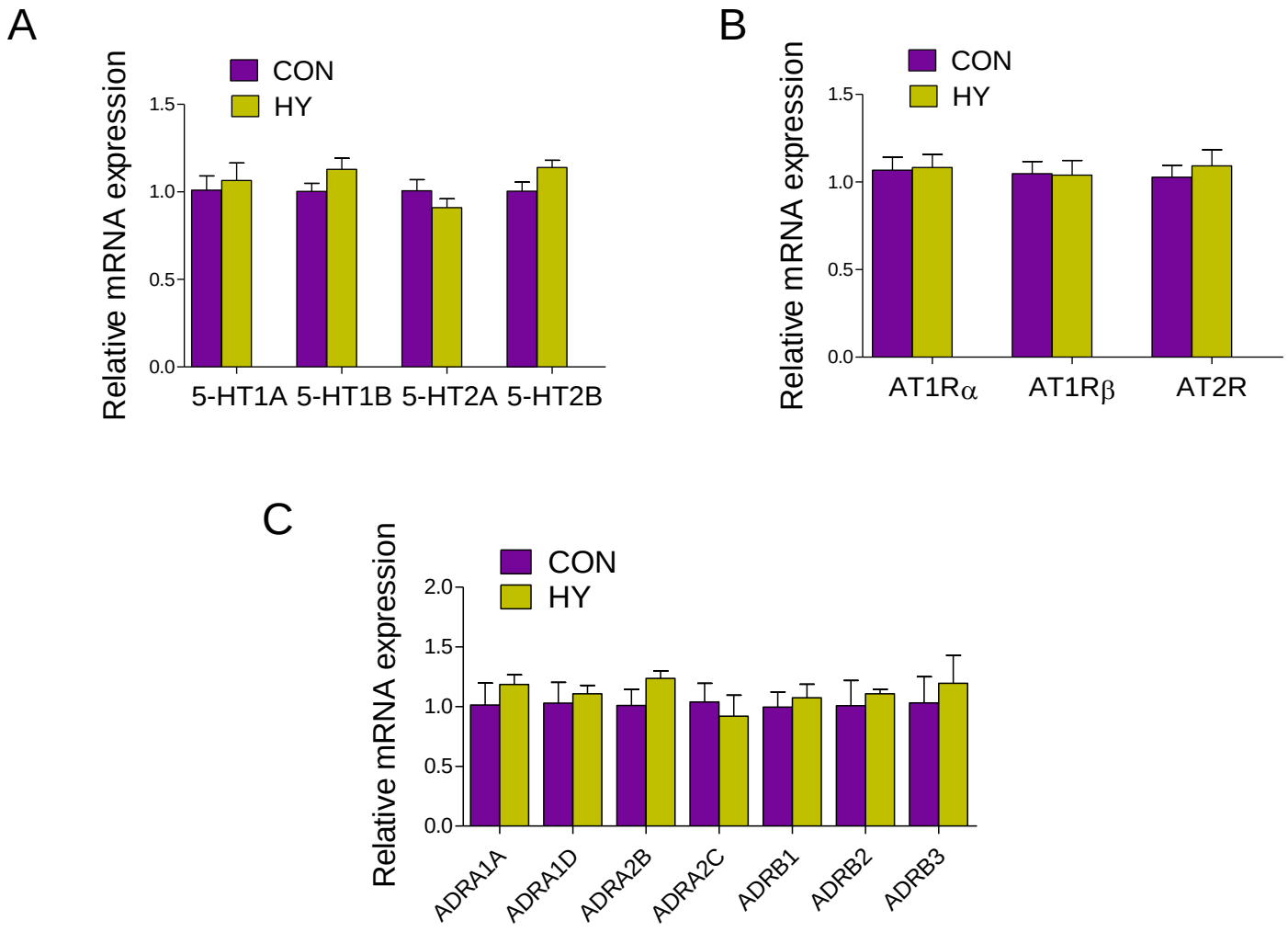

Figure S3. A-C) mRNA levels of receptors of serotonin hydrochloride (A), Angiotensin II (B) or phenylephrine (C). Results are mean±SEM of 3-6 independent experiments.

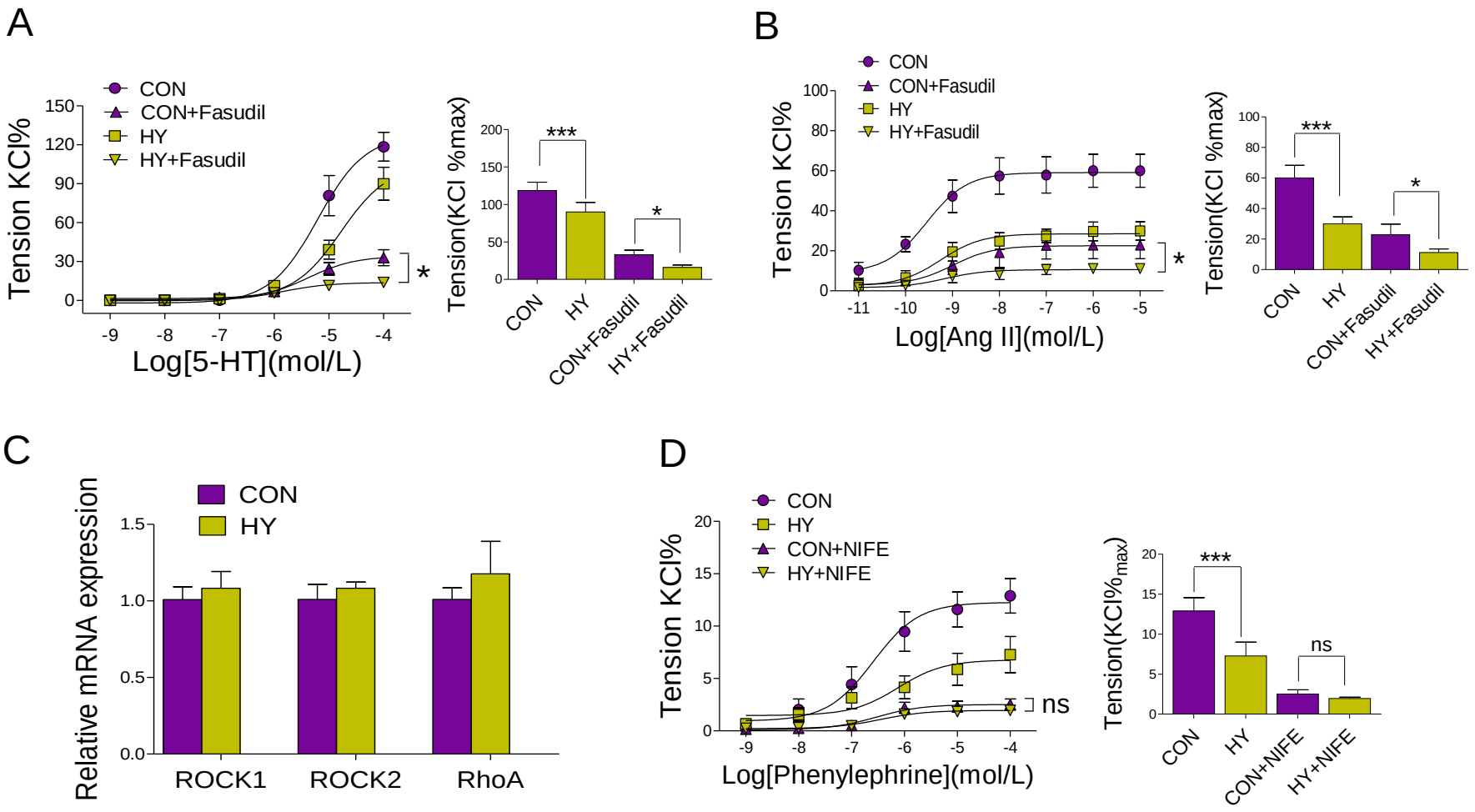

Figure S4. A and B) 5-HT or Ang II-induced contractions in the presence or absence of Fasudil (Rho/Rho-kinase inhibitor) in offspring pulmonary artery rings (N=5, n = 10). **C)** Expressions of Rho/rho-kinase (ROCK) in pulmonary artery. **D)** Phenylephrine-induced contractions in the presence or absence of NIFE (Nifedipine, antagonist for LTCCs) in offspring pulmonary artery rings (N=5, n = 10). Data were presented as means ±SEM. N, number of male adult offspring from different litters of each group. n, number of pulmonary artery rings. Data were analyzed by Student's t test or two-way ANOVA followed by Bonferroni post-tests. *, $P < 0.05$; ***, $P < 0.001$; ns, nonsignificance.

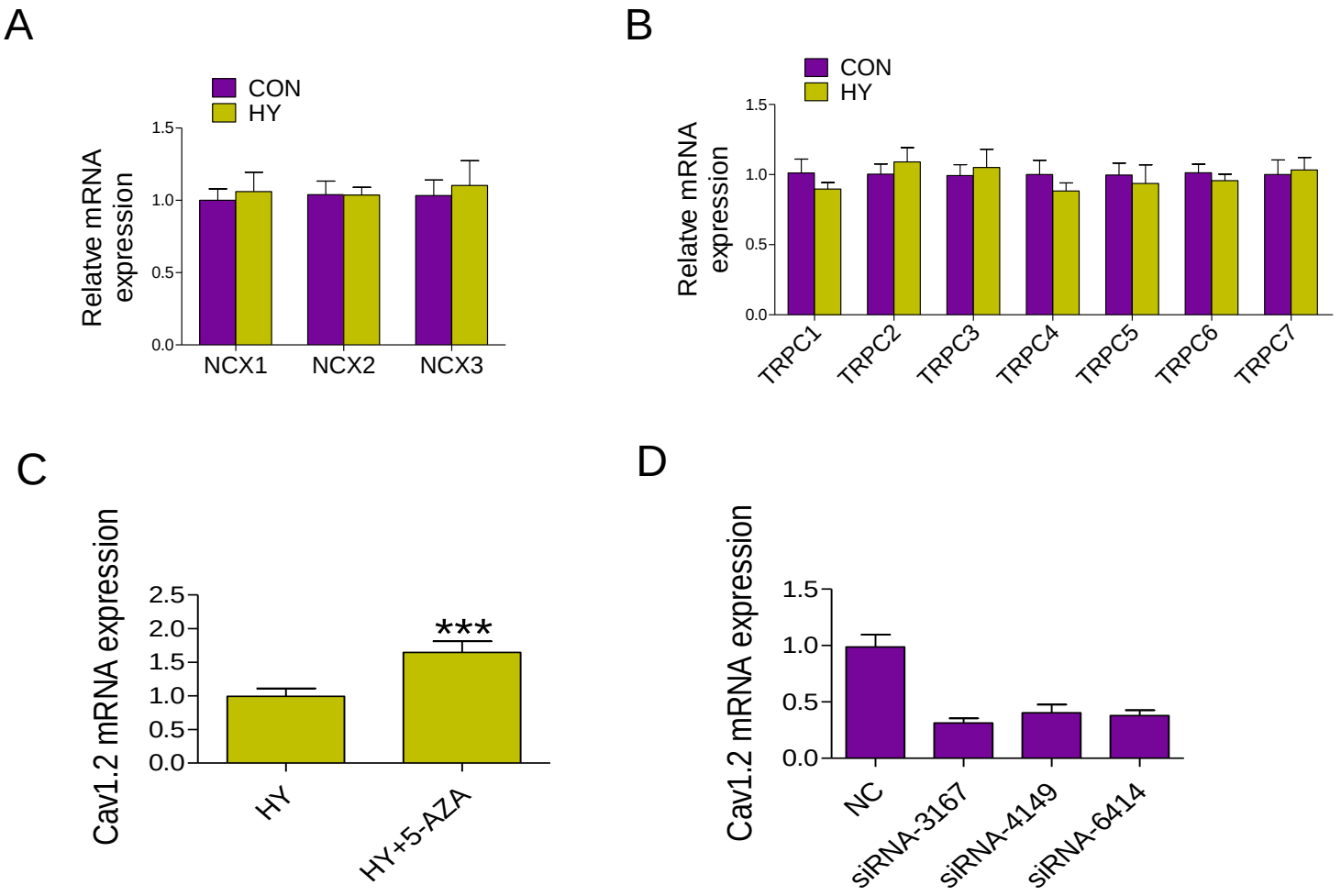

Figure S5. A and B) Expression of NCX (A) and TRPC (B) in pulmonary artery. **C)** Expression of Cav1.2 in offspring PA rings after treatment with 5-AZA (5-AZA-2'-deoxycytidine, DNA methyltransferase inhibitor). **D)** Knockdown of Cav1.2 with siRNAs was verified by qRT-PCR. Results are mean ± SEM of 3-6 independent experiments. ***, $P < 0.001$.

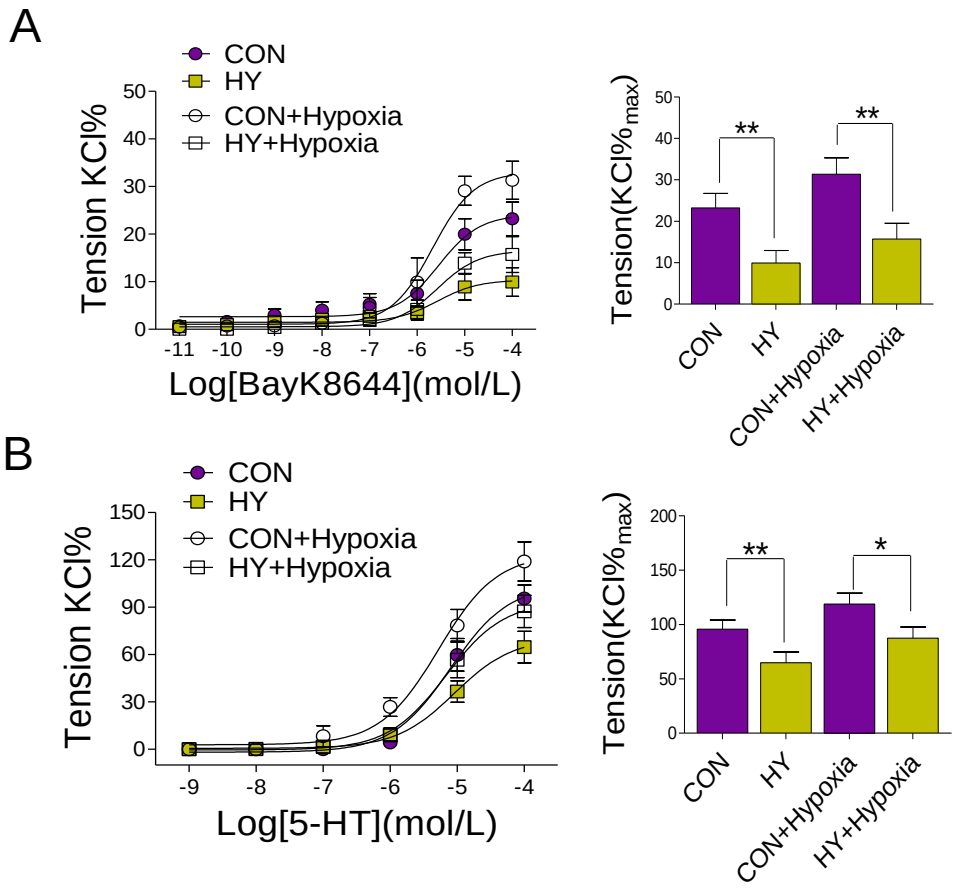

Figure S6. A and B) The effect of chronic hypoxia on BayK8644 (A) or 5-HT (B)-induced contractions in control and antenatal hypoxic offspring pulmonary artery. Control and antenatal hypoxic offspring were exposed to room air or hypoxic environment (10.5% oxygen) in a normobaric chamber. The duration of hypoxic exposure was 2 weeks, then adult male offspring were sacrificed, and pulmonary artery were isolated for vascular function assay. N=4, n=10 for each group. N, number of male adult offspring from different litters of each group. n, number of pulmonary artery rings. Data were analyzed by Student's t test. *, $P < 0.05$; **, $P < 0.01$.